

Argonne National Laboratory

QUANTITATIVE ANALYSIS OF HYDROGEN GAS FORMED BY AQUEOUS CORROSION OF METALLIC URANIUM

By

J. E. FONNESBECK



Argonne National Laboratory, Argonne, Illinois 60439
operated by the University of Chicago
for the United States Department of Energy under Contract W-31-109-Eng-38

Argonne National Laboratory, with facilities in the states of Illinois and Idaho, is owned by the United States Government and operated by The University of Chicago under the provisions of a contract with the Department of Energy.

DISCLAIMER

This report was prepared as an account of work sponsored by an agency of the United States Government. Neither the United States Government nor any agency thereof, nor The University of Chicago, nor any of their employees or officers, makes any warranty, express or implied, or assumes any legal liability or responsibility for the accuracy, completeness, or usefulness of any information, apparatus, product, or process disclosed, or represents that its use would not infringe privately owned rights. Reference herein to any specific commercial product, process, or service by trade name, trademark, manufacturer, or otherwise, does not necessarily constitute or imply its endorsement, recommendation, or favoring by the United States Government or any agency thereof. The views and opinions of document authors expressed herein do not necessarily state or reflect those of the United States Government or any agency thereof, Argonne National Laboratory, or The University of Chicago.

Available electronically at <http://www.doe.gov/bridge>

Available for a processing fee to U.S. Department of Energy and its contractors, in paper, from:

U.S. Department of Energy
Office of Scientific and Technical Information
P.O. Box 62
Oak Ridge, TN 37831-0062
phone: (865) 576-8401
fax: (865) 576-5728
email: reports@adonis.osti.gov

ANL-00/19

ARGONNE NATIONAL LABORATORY
P.O. Box 2528
Idaho Falls, Idaho 83403

**QUANTITATIVE ANALYSIS OF HYDROGEN GAS FORMED BY
AQUEOUS CORROSION OF METALLIC URANIUM**

by

Jacqueline E. Fonnesebeck

Engineering Division
Argonne National Laboratory

September 2000

TABLE OF CONTENTS

	<u>Page</u>
ABSTRACT	v
I. INTRODUCTION	1
II. THEORETICAL BACKGROUND	1
III. EXPERIMENTAL	2
IV. RESULTS AND DISCUSSION	4
A. Dissolved O ₂ and pH Measurements of the SJ-13 Water	4
B. Oxygen Depletion of the Gas Mixture in the Vessel Headspaces	6
C. Hydrogen Generation	8
D. Corrosion Rate of the DU Blanket Material	9
E. Analysis of Sample 3 Corrosion Product	10
F. Mass Balance of the Corrosion Products belonging to Samples 1,2, and 3	13
V. CONCLUSION	15
ACKNOWLEDGMENTS	16
REFERENCES	17

LIST OF FIGURES

	<u>Page</u>
Figure 1. Gas Sampling Apparatus	3
Figure 2. Cumulative Moles of Hydrogen Produced by the Three DU Samples	8
Figure 3. Uranium Corrosion Curves for the Three DU Samples	10
Figure 4. Corrosion Product from Sample 3	12
Figure 5. XRD Pattern for Sample 3 Corrosion Sludge	12
Figure 6. Stacked XRD Patterns for the Three DU Sample Corrosion Products Showing UO_{2+x} Only	14

LIST OF TABLES

	<u>Page</u>
Table 1. Chemical Additives for the SJ-13 Well Water	3
Table 2. Dissolved O_2 Data Obtained During Sampling of the SJ-13 Water	5
Table 3. pH Measurements of the SJ-13 Sample Aliquots	5
Table 4. Average Mole Percent of Air Gases Found in the Vessel Headspaces during the First Three Sampling Periods	7
Table 5. DU Corrosion Data After 81 Days	9
Table 6. Mass Balance for Sample 1 and 2 Corrosion Product	15

QUANTITATIVE ANALYSIS OF HYDROGEN GAS FORMED BY AQUEOUS CORROSION OF METALLIC URANIUM

by

Jacqueline E. Fannesbeck

ABSTRACT

Three unirradiated EBR-II blanket fuel samples containing depleted uranium metal were corrosion tested in simulated J-13 well water at 90°C. The purpose was to study the products of the aqueous corrosion of U metal i.e. UO_2 , UO_{2+x} , UH_3 , and H_2 . The corrosion products were weighed for mass balance and analyzed by x-ray powder diffraction. The data showed that UO_2 powder, as well as higher oxides i.e. UO_{2+x} had formed. However, no UH_3 was detected. The corrosion rate of uranium metal in water at 90° C was inferred by collecting and quantitatively measuring the hydrogen gas evolved.

- Figure 1: [illegible]
 Figure 2: [illegible]
 Figure 3: [illegible]
 Figure 4: [illegible]
 Figure 5: [illegible]
 Figure 6: [illegible]

- Table 1: [illegible]
 Table 2: [illegible]
 Table 3: [illegible]
 Table 4: [illegible]
 Table 5: [illegible]
 Table 6: [illegible]
 Table 7: [illegible]
 Table 8: [illegible]
 Table 9: [illegible]
 Table 10: [illegible]
 Table 11: [illegible]
 Table 12: [illegible]
 Table 13: [illegible]
 Table 14: [illegible]
 Table 15: [illegible]
 Table 16: [illegible]
 Table 17: [illegible]
 Table 18: [illegible]
 Table 19: [illegible]
 Table 20: [illegible]
 Table 21: [illegible]
 Table 22: [illegible]
 Table 23: [illegible]
 Table 24: [illegible]
 Table 25: [illegible]
 Table 26: [illegible]
 Table 27: [illegible]
 Table 28: [illegible]
 Table 29: [illegible]
 Table 30: [illegible]
 Table 31: [illegible]
 Table 32: [illegible]
 Table 33: [illegible]
 Table 34: [illegible]
 Table 35: [illegible]
 Table 36: [illegible]
 Table 37: [illegible]
 Table 38: [illegible]
 Table 39: [illegible]
 Table 40: [illegible]
 Table 41: [illegible]
 Table 42: [illegible]
 Table 43: [illegible]
 Table 44: [illegible]
 Table 45: [illegible]
 Table 46: [illegible]
 Table 47: [illegible]
 Table 48: [illegible]
 Table 49: [illegible]
 Table 50: [illegible]
 Table 51: [illegible]
 Table 52: [illegible]
 Table 53: [illegible]
 Table 54: [illegible]
 Table 55: [illegible]
 Table 56: [illegible]
 Table 57: [illegible]
 Table 58: [illegible]
 Table 59: [illegible]
 Table 60: [illegible]
 Table 61: [illegible]
 Table 62: [illegible]
 Table 63: [illegible]
 Table 64: [illegible]
 Table 65: [illegible]
 Table 66: [illegible]
 Table 67: [illegible]
 Table 68: [illegible]
 Table 69: [illegible]
 Table 70: [illegible]
 Table 71: [illegible]
 Table 72: [illegible]
 Table 73: [illegible]
 Table 74: [illegible]
 Table 75: [illegible]
 Table 76: [illegible]
 Table 77: [illegible]
 Table 78: [illegible]
 Table 79: [illegible]
 Table 80: [illegible]
 Table 81: [illegible]
 Table 82: [illegible]
 Table 83: [illegible]
 Table 84: [illegible]
 Table 85: [illegible]
 Table 86: [illegible]
 Table 87: [illegible]
 Table 88: [illegible]
 Table 89: [illegible]
 Table 90: [illegible]
 Table 91: [illegible]
 Table 92: [illegible]
 Table 93: [illegible]
 Table 94: [illegible]
 Table 95: [illegible]
 Table 96: [illegible]
 Table 97: [illegible]
 Table 98: [illegible]
 Table 99: [illegible]
 Table 100: [illegible]

I. INTRODUCTION

The effects of aqueous corrosion of metallic uranium is an important parameter in understanding the degradation of spent nuclear fuel (SNF) during interim and extended storage. Apart from the effects on radionuclide release, aqueous corrosion can produce hydrogen (H_2), a flammable gas, and uranium hydride (UH_3), a pyrophoric solid.

The results of the experiment described in this paper were used to define some of the parameters that can affect both the production of hydrogen and uranium hydride when uranium based metallic fuel comes in contact with water. These experiments involved submerging unirradiated, unalloyed uranium in water prototypic of the Yucca Mountain repository (simulated J-13 well water) and accelerating the corrosion process by raising the temperature to $90^\circ C$.

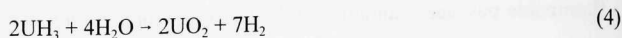
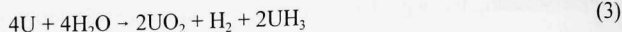
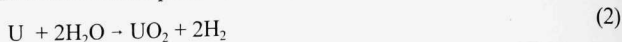
The increase of pressure within sealed vessels containing the U samples immersed in the SJ-13 water was measured over time. This information was used to determine a uranium corrosion rate using the experimental conditions described below. Gas composition was determined by Gas Mass Spectrometry (GMS) or Gas Chromatography (GC). The corrosion products were analyzed using X-Ray Diffraction (XRD) to identify the solid species which had formed during the corrosion process. The final products were also weighed for mass balance calculations.

II. THEORETICAL BACKGROUND

There are two major modes of uranium aqueous corrosion. It has been shown that for oxygenated water vapor, uranium is oxidized by O^{2-} formed from O_2 gas. This process is referred to as 'oxic' and is represented by the general reaction



The second mode is referred to as 'anoxic', by which the uranium is oxidized via hydroxyl ions formed during the hydrolysis of water at the uranium oxide surface.[1] The following reactions express the overall anoxic process,



Both the oxic and anoxic reactions most likely occur simultaneously. However, the kinetics of the anoxic reaction are much faster than the oxic one.[3] The principal difference between oxic and anoxic uranium corrosion is the formation of uranium hydride (UH_3) and hydrogen (H_2) in the latter.

Recent uranium corrosion studies of three irradiated EBR-II blanket fuel segments submerged in simulated J-13 well water showed that, after an initial slower leaching period, the rapid release of ^{137}Cs and ^{90}Sr can occur.[2] In addition, a vessel containing one of the segments became pressurized, indicating H_2 production during the periods when the vessel was isolated from laboratory air. When these tests were terminated, corrosion products from two out of the three samples contained UH_3 . The tests described below were performed with unirradiated samples to eliminate any possible effects of irradiation, and were designed specifically to quantify hydrogen evolution throughout the corrosion process.

III. EXPERIMENTAL

Three unirradiated EBR-II blanket fuel segments were sliced from a larger piece into approximately equal lengths. They each measured 1.11 cm in diameter with an average length of about 0.66 cm. Each segment was placed in a 45 mL Parr pressure vessel equipped with a gas sampling port. Into each vessel was poured enough SJ-13 well water to equal a sample surface area to leachant volume (S/V) ratio of 12 m^{-1} . The initial pH of the SJ-13 well water was 8.65 at room temperature. The SJ-13 water consisted of the compounds listed in Table 1.

Table 1. Chemical Additives for the SJ-13 Well Water

Compound	Concentration mg/L
NaHCO_3	180
KHCO_3	14
$\text{CaCl}_2 \cdot 2\text{H}_2\text{O}$	12.3
$\text{Ca}(\text{NO}_3)_2 \cdot 4\text{H}_2\text{O}$	19.8
$\text{CaSO}_4 \cdot 2\text{H}_2\text{O}$	20.6
$\text{MgSO}_4 \cdot 7\text{H}_2\text{O}$	18
$\text{SiO}_2 \cdot \text{H}_2\text{O}$	85

The sealed Parr pressure vessels were placed in a 90°C oven and allowed to accumulate internal pressure from H_2 buildup. Periodically, the vessels were sampled for gas using the apparatus shown in Figure 1. This is a photograph of the gas manifold onto which is attached a Parr pressure vessel, a 25 mL gas collection cylinder, two pressure transducers connected to a digital readout display, and an outlet for evacuating the apparatus of residual gases between sampling intervals. The pressure range for the transducers were 0-50 psig and 0-500 psig, respectively.

Initially, at each sampling interval, the vessels were opened and 4 mL aliquots of the SJ-13 water were taken for dissolved O_2 and the pH measurements. The missing leachate was then

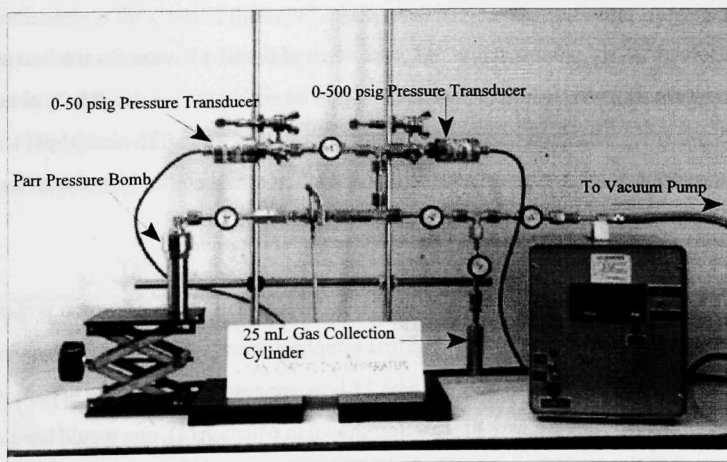


Figure 1. Gas Sampling Apparatus

replaced with fresh leachant and the vessels were recapped and again placed in the 90°C oven. The O₂ and pH measurements were discontinued after the first few sampling intervals for reasons discussed in Section V.

The H₂ that had formed was measured by either using GMS or GC. Both of these methods are highly sensitive, however GC was ultimately chosen because of the relative facility of operation as compared to GMS. The mole percent of each gas product was taken into account when calculating the partial pressure of H₂ (P_H) in the gas mixture. Upon determining the partial pressure of H₂, the number of moles of H₂ (n_H) could then be calculated using the ideal gas equation defined as

$$P_H V = n_H RT \quad (5)$$

From this data, the grams of uranium metal consumed by the corrosion process were ‘indirectly’ calculated, assuming that the reaction followed equation (2), without UH₃ formation.

IV. RESULTS AND DISCUSSION

A. Dissolved O₂ and pH Measurements of the SJ-13 Water

Dissolved O₂ and pH measurements were taken of the SJ-13 water for the first several sampling periods. In order to have a baseline to compare with these results, the O₂ concentration and the pH were also measured on a blank sample of the SJ-13 water. The initial pH was 8.65 and the O₂ level was 90.5% of air saturation ($\sim 2.3 \times 10^{-5}$ mol O₂/mol H₂O) at the current local temperature and pressure.

O₂ Measurements. Periodic oxygen levels are tabulated in Table 2 where it is shown that the O₂ levels had dropped appreciably by the first sampling period on day nine. However, percent saturation varied little (34 to 55%) over the next 21 days, suggesting that oxygen depletion was somehow incomplete. According to the reaction shown in equation (1), one would have expected the O₂ levels to continue to decline until all of the O₂ was consumed. The only conclusion drawn

Table 2. Dissolved O₂ Data Obtained During Sampling of the SJ-13 Water

Day	Sample 1		Sample 2		Sample 3	
	%O ₂	mg O ₂ / g H ₂ O	%O ₂	mg O ₂ / g H ₂ O	%O ₂	mg O ₂ / g H ₂ O
9	39.1	1.8E-2	33.5	1.5E-2	35.3	1.6E-2
14	54.9	2.5E-2	46.3	2.1E-2	47.0	2.1E-2
21	NA	NA	NA	NA	36.0	1.6E-2

from these observations was that, although precautions were taken to avoid exposing the leachates to air during sampling intervals, they nonetheless rapidly absorbed atmospheric O₂, resulting in erroneously high levels. To test this hypothesis, the O₂ uptake of deaerated water in laboratory air was monitored. The rate of O₂ uptake was fairly rapid at 1.5×10^{-3} mg O₂/g H₂O/min or a 3.3% O₂ saturation increase per minute (at 635.8 Torr and 12°C). This result showed that although O₂ depletion of the leachant had occurred during the time interval between sampling periods, quantitative data could not be collected unless the environment was completely isolated from oxygen. Due to this experimental obstacle, O₂ measurements were abandoned beyond day 21.

pH Measurements. The results from the pH measurements are shown in Table 3. The pH rose significantly at the onset of the experiment and remained fairly constant afterwards. This phenomenon was addressed by assessing the reason for the increase in pH, i.e. basicity. The dynamics behind the change in pH could only be attributed to chemical events occurring within the vessels. These events definitely include the reactions expressed in equations 1-4 and could possibly include other 'side' reactions involving the ionic species in the SJ-13 water itself, namely

Table 3. pH Measurements of the SJ-13 Sample Aliquots

Day	pH of SJ-13 Aliquots (initial = 8.65)		
	Sample 1	Sample 2	Sample 3
9	9.95	10.21	10.02
14	10.38	10.21	9.92
21	NA	NA	9.84
23	10.38	10.38	9.87
81	NA	NA	9.79
119	10.30	10.35	NA

the slightly acidic bicarbonate anion (HCO_3^-). The bicarbonate anion is known for its buffering effect in aqueous media. This occurs when both the bicarbonate anion and its conjugate base, CO_3^{2-} , are close to equal concentrations. This conjugate acid/base pair is resistant to changes in pH. The condition is mathematically expressed as follows:

$$\text{pH} = \text{pK}_{a2} + \log [\text{CO}_3^{2-}]/[\text{HCO}_3^-] \quad (6)$$

where the pK_{a2} is the log of the acid dissociation constant K_{a2} for H_2CO_3 . So the buffering capability of this system is maximum when $[\text{CO}_3^{2-}] = [\text{HCO}_3^-]$ and the above equation becomes $\text{pH} = \text{pK}_{a2}$. Incidentally, the pK_{a2} for CO_3^{2-} is 10.33 which is very close to the pH readings taken of the leachates.

In order for the buffering to occur, a strong base had to be added until the above conditions were met. One possible explanation for this phenomenon could involve a fairly well studied mechanism which occurs during uranium metal aqueous corrosion. During the process of forming UO_2 , hydroxyl (OH^-) ions are also produced via the hydrolysis of water.[1,3] The formation of OH^- ions in the SJ-13 could explain the increase in pH. The change in the observed pH indicates that enough hydroxyl anions had been produced to reach the maximum buffering capacity of the $\text{HCO}_3^-/\text{CO}_3^{2-}$ equilibrium where $\text{pH} = \text{pK}_{a2}$. This reaction is shown in the following equation:



Hence, the OH^- ions produced provided the impetus to drive reaction (7) above to the right, thereby increasing the CO_3^{2-} concentration.

B. Oxygen Depletion of the Gas Mixture in the Vessel Headspaces

The pressure changes in the vessels were measured over time and the gas product was analyzed for the first three sampling intervals by GMS. All gas samples were ultimately analyzed by GC. During the first two sampling intervals (day 9 and 14), the three vessels were

opened in order to obtain aliquots of the SJ-13 water (for both the pH and the dissolved O₂ measurements). On day 21, the third vessel alone was opened for sampling. And, again on day 23, all three vessels were again opened to obtain leachate samples. The first several gas sampling intervals revealed that the gas product consisted of several constituents of which hydrogen was the major component. Nitrogen, oxygen, and trace argon which are gases normally found in air, were also detected. This was not surprising considering the leachates came in contact with air each time aliquots were taken for pH and dissolved O₂ measurements. However, after leachate sampling was terminated, these other gases were eventually diluted down to non-detectable limits. From then on, hydrogen was the only accountable gas present in the gas product.

Table 4 shows the average O₂, N₂, and Ar mole percent values and the O₂/N₂ and Ar/N₂ ratios obtained from the first three gas sampling intervals. The O₂/N₂ ratios found in the gas samples were significantly lower than normally found in air which is approximately 0.256. The Ar/N₂ found in the gas samples were close to the normal air ratio of 0.012. What appears to have occurred was that the O₂ had been 'removed' from the headspace above the leachates. This data is evidence that O₂, which was reintroduced into the vessels when opened for leachate sampling, was being absorbed by the leachate and, in turn, reacting with the uranium metal.

As above mentioned, gas samples were drawn throughout the experiment in order to measure the mole percent of hydrogen. Over time, the other gases were diluted out resulting in a gas product that approached 100 % hydrogen.

Table 4. Average Mole Percent of Air Gases Found in the Vessel Headspaces during the First Three Sampling Periods

Day	Average Mole Percent Measured			Average O ₂ /N ₂	Average Ar/N ₂
	O ₂	N ₂	Ar		
9	0.02	6.23	0.08	0.003	0.013
14	0.00	3.80	0.06	0.000	0.016
21	0.01	1.85	0.03	0.005	0.016

C. Hydrogen Generation

Figure 2 shows the quantity of hydrogen produced throughout the course of the experiment. Notice that the H_2 product from Samples 2 and 3 correlated quite closely, whereas Sample 1 was slightly higher. After day 9, H_2 production in Sample 1 was 50 % greater than in either Sample 2 or 3. However, by day 81, the accumulated amount of H_2 produced by Sample 1 exceeded Sample 2 by 14 % and Sample 3 by 19 %. The discrepancy between the average rate of H_2 production between Samples 2 and 3 and Sample 1 was diminishing with time.

Gradually, the cumulative H_2 production for all 3 samples was approaching the same value such that, by day 119 the difference between Sample 1 and 2 was only 4 %. This comparison could not be made with Sample 3 on day 119 because its final gas sampling interval was on day 81. However, since the rate of Sample 3 was essentially identical to that of Sample 2 it is assumed that the behavior of Sample 3 would have continued to behave like Sample 2. Sample 3 was removed from the test at day 81 for characterization of a partially reacted sample. Meanwhile, tests on Samples 1 and 2 were left to react until appreciable pressure increases could

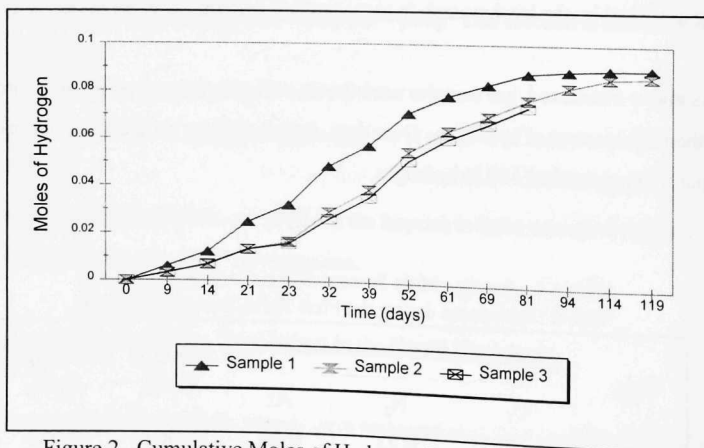


Figure 2. Cumulative Moles of Hydrogen Produced by the Three DU Samples

no longer be measured suggesting the samples had completely reacted. Figure 2 shows how the curves had almost leveled off by day 119.

D. Corrosion Rate of the DU Blanket Material

The mass of uranium metal that had reacted in each sample was derived from the H_2 gas pressure measurements. These calculations assumed all of the hydrogen produced was in the gas form (H_2) rather than as the hydride (UH_3) as represented by equation (2) and neglected the small pressure contribution from other gasses. The results are listed in Table 5. After 81 days, it can be seen that, on average, three-quarters of the total uranium in these samples had corroded. To reiterate, these values are based upon the assumption that the only compound present in the reaction product was stoichiometric UO_2 only. They do not include the quantity of uranium metal that may have reacted to form UH_3 . If any hydrogen was present in the form of UH_3 , then the total metal corroded would be higher than the calculated uranium values listed in Table 5. However, it is impossible to quantify UH_3 from the H_2 data alone. As it turned out, there was no hydride in the corrosion product, however, this will be discussed in more detail in Section E.

Figure 3 represents the uranium corrosion mass curves for the three samples. The straight line shown was derived from the least-squares fit of the averaged uranium corrosion curves of the three samples. The slope of this line can be interpreted as the average rate at which the uranium had corroded. The rate was $34 \text{ mg/cm}^2/\text{day}$.

Table 5. DU Corrosion Data After 81 Days

Sample #	Original Mass (grams)	Calculated Mass of Uranium Oxidized	Percent of Sample Oxidized
1	11.996	10.5	87.5
2	12.029	9.2	76.5
3	11.123	8.8	79.1

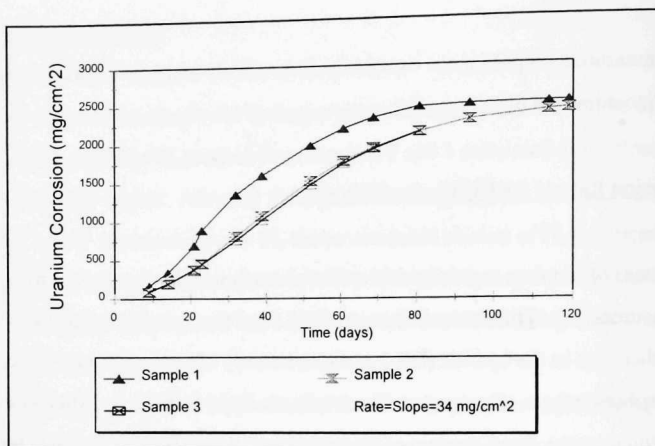


Figure 3. Uranium Corrosion Curves for the Three DU Samples

Only the averaged data from day 9 through day 69 were included in the derivation of the regression curve because the H_2 production rate remained fairly constant during this time frame. Beyond day 69, the rate began to decline as shown by the graphed data. This decline is attributed to the decreasing sample size (surface area) which was assumed constant.

The corrosion rate of uranium metal obtained from this work corresponds very closely to a compilation of uranium corrosion rates reported for immersion studies in anoxic water.[4] A linear regression fit to the published data yielded the following Arrhenius expression

$$\ln k = 22.34 - 7989/T \quad (8)$$

where k is the U corrosion rate constant in $mg\ U/cm^2/hr$, and T is the temperature in Kelvin. For $90^\circ C$, equation (8) predicts a corrosion rate of $1.4\ mg/cm^2/hr$, which is in good agreement with the experimental reaction rate ($1.42\ mg/cm^2/hr$) derived from the H_2 data in this study.

E. Analysis of Sample 3 Corrosion Product

Day 81 was the final gas sampling interval for the vessel containing sample number 3.

Figure 3 shows that the uranium corrosion rates were essentially identical for both samples 2 and 3. Based upon this observation, the corrosion rate experiment was terminated early for Sample 3. In a previous corrosion study of irradiated EBR-II blanket fuel, three samples contained UO_2 , but only two contained UH_3 . [2] Interestingly, the sample whose corrosion sludge showed only UO_2 , was that which had completely corroded. As for the other two, there remained some unoxidized uranium metal. Since UH_3 is an intermediary product in the anoxic process, observing a correlation between the existence of UH_3 in the presence of uranium metal and its absence when uranium metal is no longer present was a point of interest for the current experiment.

After the contents of the Sample 3 vessel had been filtered through a glass fiber filter, its visual appearance in the wet condition was that of a dark, brown, clay-like substance. However, after drying in ambient air for several days, the product was predominately a fine, black powder. A portion of this material can be seen in Figure 4. While most of the sample consisted of the black powder, there were pieces of agglomerated chunks which could be easily broken up. A very small piece of the original metallic sample remained. This is consistent with the data in Table 5 since the calculations indicated that less than 13% of the original sample remained. However, the remaining sample retained its original cylindrical geometry and was completely covered by a solid black coating.

A small portion of the black powder (about 40 mg) was taken and further pulverized to a fine powder. This small sample was submitted for XRD analysis to determine the phases present within this product. The instrument used for XRD analysis was a Scintag X1 powder diffractometer. This instrument utilized Cu K_α x-radiation at an average wavelength of 1.5418 Å. The 2θ scan ranged from 20° to 75° .

The resulting diffraction pattern shown in Figure 5 indicates that the corrosion product contained UO_{2+x} or possibly a mixture of both UO_2 and U_3O_7 . Since the diffraction lines are so broad, it is difficult to determine whether this broadening was due to the presence of UO_2 alone. However, the diffraction peaks are seen to be shifted to lower d spacings, i.e. greater 2θ , than stoichiometric UO_2 , indicating an oxygen to metal ratio greater than 2.0. This shift can be seen



Figure 4. Corrosion Product from Sample 3

in Figure 5 which shows that the apex of the diffraction 'peaks' are located slightly to higher 2θ than the true Bragg lines indicated for UO_2 .

No uranium hydride, uranium oxy-hydrates, or uranium metal diffraction peaks were present, indicating the loose powder was strictly UO_2 or UO_{2+x} . This was consistent with Gray,

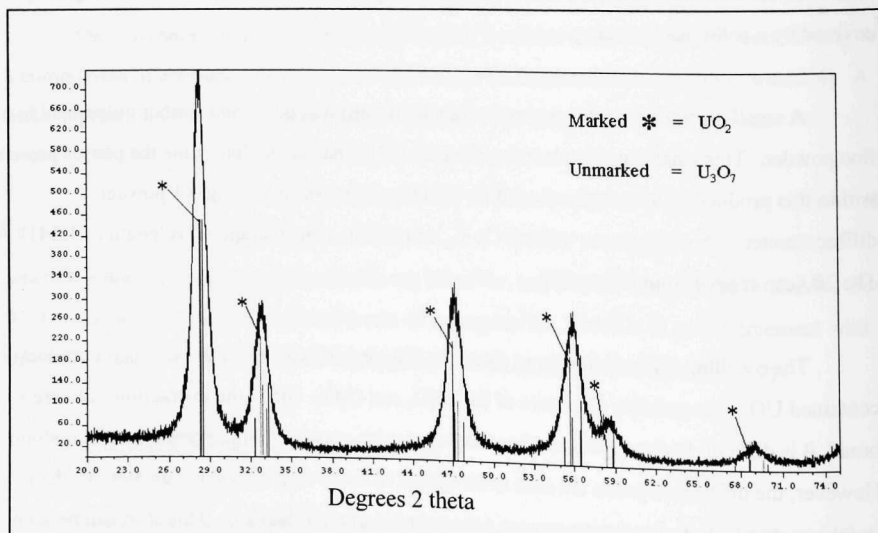


Figure 5. XRD Pattern for Sample 3 Corrosion Sludge

who reported only UO_2 product from the N-Reactor spent fuel flowthrough tests.[5] Yet others have reported the presence of UH_3 in the uranium aqueous corrosion product.[2,6] It is not yet understood why uranium corrosion product sometimes contains UH_3 , and other times none.

F. Mass Balance of the Corrosion Products belonging to Samples 1,2, and 3

Sample 3 Prior to the XRD analysis, all of the solid material was weighed after drying. The final weight was 12.4 g (See Table 6). As indicated from the XRD pattern in Figure 5, the corrosion product contained no hydride. Therefore, all of the uranium that had reacted should have converted to either UO_2 or a mixture of UO_2 and a higher oxide such as U_3O_7 . However, since some of the original uranium metal was yet intact, it was difficult to determine through weight gain alone which and how much product had formed. To simplify the mass balance issue, it was assumed that all of the uranium metal that had reacted was converted to UO_2 only. The following mass numbers were obtained from the uranium corrosion rate curve which was, in turn, derived from the raw data obtained from the hydrogen measurements. Hence, by day 81 (Table 5), 8.8g of the original 11.12 g of uranium metal was calculated as being oxidized. Assuming the uranium metal reacted with water to form stoichiometric UO_2 , the added oxygen would have been equal to 1.18 g, thus increasing the total mass of the sample to 12.30 g. The difference between the weighed value (12.4 g) and the value derived indirectly by the gas data (12.30g) is less than 1.3%. One reasonable explanation for the greater mass exhibited by the weighed value could be have been due to the presence of higher oxides i.e. UO_{2+x} , etc. As shown below, Samples 1 and 2 provide more reliable weight gain data with which to ascertain the oxidation state.

Samples 1 and 2 Pressure measurements continued to be taken from vessels 1 and 2 until the hydrogen production rate slowed sufficiently to flatten out the curves as plotted in Figure 3. The final gas samples were taken 119 days into the experiment. At this time, the two remaining vessels were uncapped and the pH of the SJ-13 water was measured. Table 3 shows that, as with Sample 3, after the initial increase, the pH remained fairly constant for the remaining two sample leachates.

The two samples were set aside in their vessels for another 52 days at ambient temperature and pressure. This would allow any remaining U metal to oxidize. The corroded material was filtered through a glass fiber filter and allowed to dry in open air for approximately 24 hours before weighing. By this time, no visible trace of metal could be found in either sample. The appearance of this material was identical to that of Sample 3, a finely divided black powder.

XRD patterns were obtained for Samples 1 and 2 and compared to that of Sample 3. Figure 6 shows the diffraction patterns for the three sample products vertically offset for comparison purposes. They are essentially identical showing only the phases belonging to some form of uranium oxide i.e. UO_{2+x} . There are no UH_3 nor uranium metal phases present within any of the three patterns.

Table 6 compares the mass of the original DU sample with the final mass of the corrosion product at the end of the experiment for Samples 1 and 2. Also shown, are the calculated

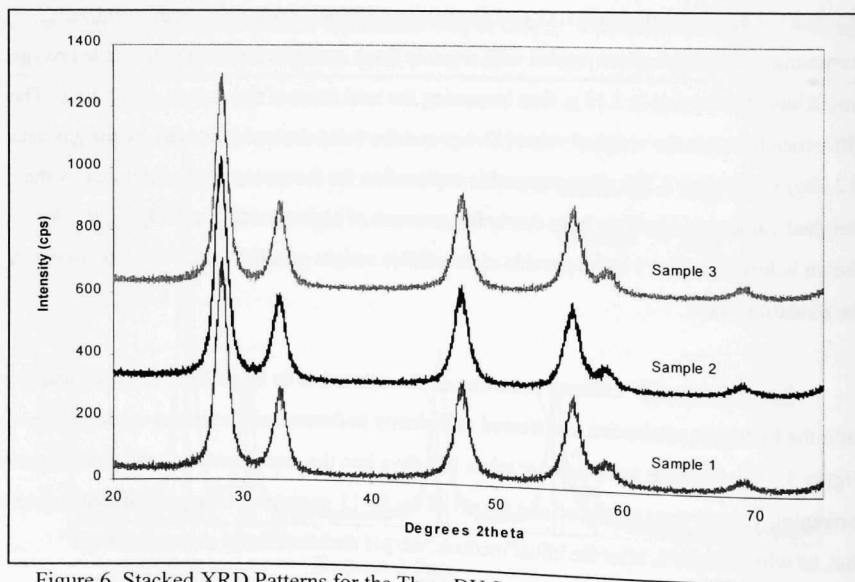


Figure 6. Stacked XRD Patterns for the Three DU Sample Corrosion Products Showing UO_{2+x} Only

Table 6. Mass Balance for Sample 1 and 2 Corrosion Product

Sample #	Initial Mass (g)	Final Mass (g)	Calculated Total UO ₂ Mass (g)	Calculated Total U ₃ O ₇ Mass (g)
1	11.996	13.99	13.61	13.88
2	12.029	14.06	13.65	13.92

corrosion product masses assuming stoichiometric conversion to either UO₂ or U₃O₇.

Table 6 shows that the actual corrosion product weighs slightly more than either of the calculated values. Attributing all of the weight gain only to an increase in oxygen content, results in oxygen/uranium ratios (O/U) for Sample 1 and 2 corrosion products of 2.47 and 2.52, respectively. Both of these values are higher than the calculated O/U for U₃O₇ (2.33) yet lower than that for U₃O₈ (2.67). Reference 7 states that U₃O₇ and U₃O_{8-x} phases can form at 90°C which brackets the U/O ratios 2.47 and 2.52.

The XRD patterns of Sample 1 and 2 corrosion products have the same shift to higher 2 θ as seen in the diffraction pattern of Sample 3. This shift of phases supports the 'higher' oxide hypothesis. However, it is difficult to unequivocally determine which oxides are present and in what quantity due to the unresolvable nature of the broad Bragg lines in the diffraction patterns.

V. CONCLUSION

It has been shown that depleted, unirradiated uranium metal undergoes rapid oxidation in 90°C water. An average uranium corrosion rate of 1.42 mg/cm²/hr in anoxic water was measured in these experiments and is essentially identical to the best fit literature value of 1.4 mg/cm²/hr for anoxic uranium corrosion reported in reference 4. This reaction rate was derived from measurements of the hydrogen gas that had evolved, assuming no UH₃ was formed as a long-term intermediate product.

The uranium product was weighed to determine mass increase. This information, plus

that gained from x-ray diffraction analysis of the corrosion product, was used to assist in the identification of the product itself. First, it was shown that no hydride was present. Second, even if no UO_2 was present at the time the diffraction patterns were acquired, certainly, oxides of the UO_{2+x} type were present. Furthermore, the mass differential between the initial sample and the final product indicated that some form of UO_{2+x} or mixtures of this formula type were present in the corrosion product of all three samples.

ACKNOWLEDGMENTS

This work was supported by the U.S. Department of Energy, Reactor Systems, Development and Technology, under contract W-31-109-Eng-38 and U.S. Department of Office Contract DE-AC07-94ID13223. Special thanks goes to several individuals at Argonne National Laboratory-West for their assistance including Dr. Robert Pahl, Paul Hart, Jeff Berg, Dan Cummings, and Dr. Steven Frank.

REFERENCES

- [1] C.A. Colmenares, "Oxidation Mechanisms and Catalytic Properties of the Actinides", *Prog. Solid St. Chem.*, **15**, 257 (1984).
- [2] J. E. Fonnesebeck, J. R. Krsul, S.G. Johnson, "EBR-II Blanket Fuel Leaching Test Using Simulated J-13 Well Water," *Proc. Third Topical Meeting on DOE Spent Nuclear Fuel and Fissile Materials Management*, Charleston, SC, September 8-11, 1998, **2**, p. 715, American Nuclear Society, La Grange Park, Illinois (1998).
- [3] S. Orman, "Oxidation of Uranium and Uranium Alloys," *Physical Metallurgy of Uranium Alloys*. J.J. Burke, ed. 815-833, Brook Hill Publishing Company (1974).
- [4] B. Hilton, "Review of Rates of Reaction of DOE Spent Nuclear Fuel in Oxygen, Water Vapor, and Water. PART I" Report No. NSNF-195 (2000). IN PRESS.
- [5] W.J. Gray and R.E. Einziger, "Initial Results from Dissolution Rate Testing of N-Reactor Spent Fuel Over a Range of Potential Geologic Repository Aqueous Conditions", DOE/SNF/REP-022 Rev 0, PNNL-11894, UC-802, Washington (1998).
- [6] T.C. Totemeier, R.G. Pahl, S.L. Hayes, S.M. Frank, "Metallic Uranium ZPPR Fuel: Corrosion Characteristics and Corrosion Product Oxidation Kinetics", Argonne National Laboratory, Idaho Falls, Idaho (1997).
- [7] L.E. Thomas, R.W. Knoll, L.A. Charlot, J.E. Coleman, E.R. Gilbert, "Microstructural Characterization of Low-Temperature Oxidized LWR Spent Fuel", PNL-6640-vol 2, December 1989.

